2017 International Nuclear Atlantic Conference - INAC 2017
Belo Horizonte, MG, Brazil, October 22-27, 2017
ASSOCIAÇÃO BRASILEIRA DE ENERGIA NUCLEAR – ABEN

Agência Brasileira do ISBN
ISBN 978-85-99141-07-6
9 788599 141076

COMPOSITES WITH CARBON NANOTUBE FOR RADIATION SHIELDING APPLICATION

Críssia C. P. Fontainha[1], Modesto Nunes [1] , Víctor A. Rosas[1], Adelina P. Santos[2], Clascídia A. Furtado[2] and Luiz O. Faria[2]

[1] Depto. de Anatomia e Imagem (IMA) – Faculdade de Medicina
Universidade Federal de Minas Gerais
Av. Prof. Alfredo Balena, 190
30130-100 Belo Horizonte, MG, Brasil
crissia@gmail.com
[2] Centro de Desenvolvimento da Tecnologia Nuclear (CDTN/CNEN)
Av. Antônio Carlos 6627, C.P. 941,
30270-901 Belo Horizonte, MG, Brazil
farialo@cdtn.br

ABSTRACT

Polymeric composites filled with attenuating metals and functionalized with carbon nanotubes (NTC) are being largely developed. New attenuators materials have been widely investigated for radiation shielding to apply in procedures as interventional radiology, Computed Tomography (CT) and nuclear medicine. In this work composites for radiation attenuation in radiodiagnostic imaging procedures made of inorganic material as filler, by a sol–gel method, in poly(vinilidene fluoride-tryfluorethylene) [P(VDF-TrFE] copolymers that are used as the polymeric matrix. Two different metal attenuators were used as fillers: zirconia stabilized by yttria (8% wt.) and bismuth oxide. Carbon nanotubes were added with different concentrations at the solution of attenuator metal under controlled magnetic stirring. Characterization of composites by FTIR, UV-Vis, DSC and SEM-EDS were carried out. In a previous analysis of radiation attenuation, was used an incident monochromatic X-ray beam from the RIGAKU diffractometer. In this setup, one reference measure is directly exposed to the x-rays being diffracted by single crystal of Si (111). Another measure the attenuated beam is performed with the composite sample under detector. The functionalization of the carbon nanotube of multiple walls (MWNCT) in the in the P(VDF-TrFE) was evaluated. The samples present a good dispersion of the attenuator metal into presence at methacrylic acid. The cheaptube presented better dispersion in the polymer matrix than the 3100 nanotubes. Bismuth oxidation composites showed a better attenuation factor compared to Zirconia stabilized by yttria composites

1. INTRODUCTION

Medical imaging examinations offers great benefit to patients, however, there is a worrying exposure of workers, patients and individuals to radiation doses, significantly increasing the average dose to population [1,2,3,4]. Procedures as interventional radiology, Computed Tomography (CT) and nuclear medicine provide high doses to the skin of patients, provoking radiation deleterious effects, because they involve long periods of direct X-ray beam pointing to the same skin region. In this context, new composites materials with attenuation features and containing compounds or elements such as barium sulfate, copper, gadolinium, gold, lead, molybdenum, rhodium, silver, tungsten, bismuth, zirconium oxide, iron oxide and zinc have been widely investigated for radiation shielding in those regions of high risk, allowing significant dose reduction near the patient's skin [5,6,7].
One of the promising future applications of carbon nanotubes (NTCs) or graphene-based nanocomposites is in the field of X-ray attenuation. Polymer composites are being developed

with NTC, presenting strong interactions between matrix and the filler, resulting in a nanometric structure with large interfacial area. The tubular structure of carbon nanotubes (NCT's) induces a significant fluctuation of the electron population across the carbon tube wall, which may favor the absorption of X-rays, by increasing the polarization factor [8,9]. Enhanced X-ray shielding effects of carbon nanotubes (CNTs) has been reported by Fujimore et al. (2011), when compared with highly oriented pyrolytic graphite (HOPG). They also demonstrated that CNT-coated fabrics could efficiently absorb 17.5 keV X-ray photons by using polyester fibers coated with only 8% of MWCNT [8]. Recently, a graphene oxide (GO)-based polymer composite has been reported to show increasing X-ray attenuation efficiency for photons with energy bellow 22.1 keV [10].
In this work, polymer-based composites were synthesized containing zirconia and bismuth oxide with two types of multi-walled carbon nanotube (MWNCT), the nanocil NC3100 and the cheaptube. The poly(vinilidene fluoride-tryfluorethylene) [P(VDF-TrFE] copolymers were used as the polymer matrix. In the synthesis process, surface modifiers were used in order to obtain better interaction between the matrix and the filler material. These composites were characterized and studied aiming application as attenuating materials in high dose medical procedures.

2. MATERIALS AND METHODS

2.1. Synthesis of composites and Structural Characterization

The synthesis of the composites involves the dispersion of metal particles in the P(VDF-TrFE) host matrix in two concentrations MWCNT's under magnetic stirring. The composites films were produced from *casting*. Figure 1 shows the flowchart of the synthesis for the composite filled with nanoparticles of bismuth oxide.

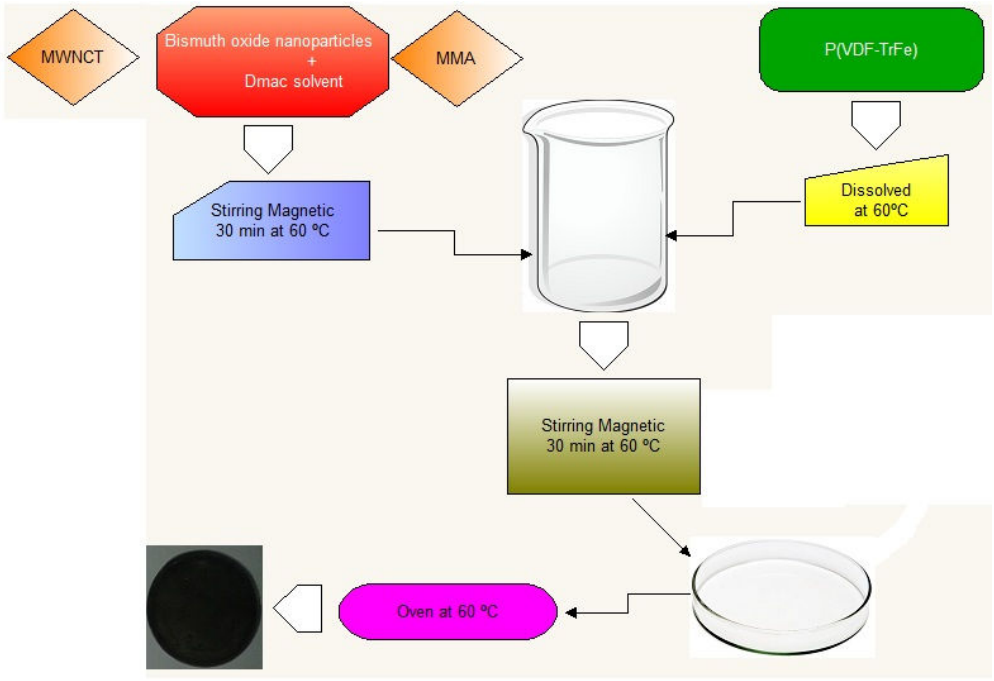

Figure 1: Flowchart of the synthesis for the composite P(VDF-TrFe) matrix filled with bismuth oxide nanoparticles.

Poly(vinylidene fluoride – trifluorethylene) copolymer [P(VDF-TrFE)$_{50/50}$] acquired from Sigma Aldrich was dissolved in DMAc (n,n-dimethylacetamide). Metallic oxides with good attenuation features were used: nanoparticulated bismuth trioxide (Bi_2O_3) 99.8% pure from Sigma Aldrich, and Zirconia stabilized by yttria (ZrO_2:8%Y_2O_3) supplied by the Laboratory of Chemistry of Nanostructured Carbon Materials of the CDTN / CNEN. Polymer based composites containing methacrylic acid (MAA), from Sigma Aldrich, and functionalized Bi_2O_3 nanoparticles and ZrO_2:8%Y_2O_3 microparticles were prepared with 10:1 concentration. The nanotubes used were NC3100^{TM} and cheaptube MWNCT's, dissolved in DMAc and dimethylformamide (DMF), in the proportion of 0.5%. The MWNCT's were shaken in a incubator with controlled speed and temperature for at least one hour prior to the syntheses. Then they were poured into the solution at 0.25 and 0.75 wt % concentrations. Surface-modified metallic particles were added to the solution matrix with concentrations of 8 wt %. Semi-transparent films were obtained after solvent evaporation at 60°C.
UV-Vis spectrophotometry were measured in order to evaluate the sample optical transparence. Thermal behavior studies were made by using a DSC TA Q10, with heating and cooling rates of 10 °C/min, in the second run, from 25 to 200 °C. The composite samples were analyzed by the Carl Zeiss field-emission scanning electron microscope (FE-MEV), Sigma VP model, at the CDTN / CNEN Scanning Electron Microscopy Laboratory (SEM). SEM analysis allowed to know the microstructure of the polymer phase and filler material.

2.1.1. X-ray Shielding Characterization

The radiation shielding characterization was performed using an incident monochromatic X-ray beam with photon energy of 8.047 keV, obtained by using the same experimental setup described by Fujimore et al.(2011) [8]. In order to generate a monochromatic incident X-ray beam, a non monochromatic X-ray was first directed to a single crystal of Si(111). The constructive diffraction from the CoKα were obtained at 2θ approximately equal to 33.13°. In order to determine the radiation attenuation for monoenergetic photons we have exposed P(VDF-TrFE) composites with Bi_2O_3 and ZrO_2:Y_2O_3 to X-rays. The beam percentage attenuation (At%) is given by formula 1:

$$At(\%) = \left(1 - \frac{I}{I_0}\right) \times 100 \qquad (1)$$

where I_0 is the intensity of the X-ray beam and I is the X-ray intensity of the attenuated beam.

RESULTS AND DISCUSSION

3.1. Characterization of composites

The sample photographs of the synthesized composites made of P(VDF-TrFE) matrix filled with the metallic oxides ZrO_2:Y_2O_3 and Bi_2O_3, with and without MWNCT, are shown in Figure 2. The polymer matrix favors a good dispersion of the attenuator metal and plasticity to the composite sample. In both samples it is possible to observe that there are no visible particle clusters, which means that the presence of MMA, at least at a macroscopic level, favors a good homogeneous distribution of attenuator metal particles into the polymeric matrix. However, some nanotubes did not show homogeneity due its dispersion, in specially

the 3100 MWCNT. On the other hand, there were better dispersed with the presence of the nanotube.

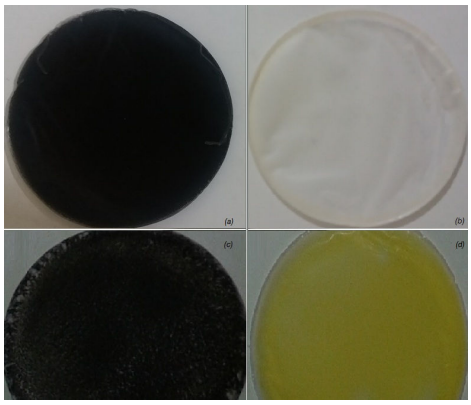

Figure 2: Synthesized composites: *(a)* P(VDF-TrFE)/ZrO_2:Y_2O_3/MMA/MWNCT, *(b)* P(VDF-TrFE)/ZrO_2:Y_2O_3/MMA, *(c)* P(VDF-TrFE)/Bi_2O_3/MMA/MWNCT, *(d)* P(VDF-TrFE)/Bi_2O_3/MMA.

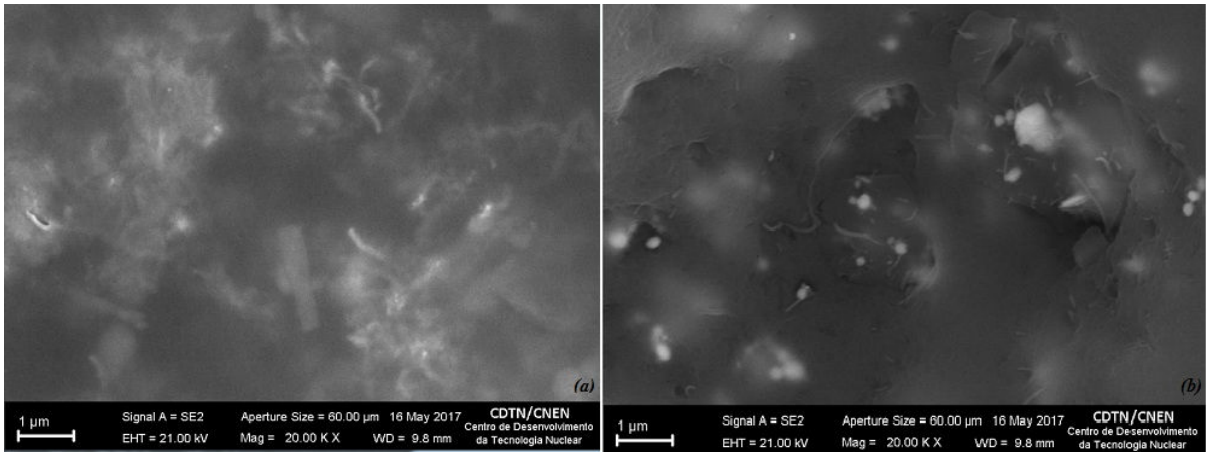

Figure 3: Micrographs of composites filled with carbon nanotube: *(a)* P(VDF-TrFE)/ZrO_2:Y_2O_3/MMA/MWNCT, *(b)* P(VDF-TrFE)/Bi_2O_3/MMA/MWNCT.

SEM analysis allowed to evaluate the state of dispersion of the agglomerates of the particulate of the attenuators metals, Figure 3. The morphological patterns of the cheaptube MWNCT found in the composites matrix were presented in micrographs. In the Figure 3 shows the entanglements of nanotubes scattered in the composite matrix, in *(a)* P(VDF-TrFE)/ZrO_2:Y_2O_3/MMA/MWNCT composite and *(b)* P(VDF-TrFE)/Bi_2O_3/MMA/MWNCT composite on the scale of 1 µm for the same magnification.

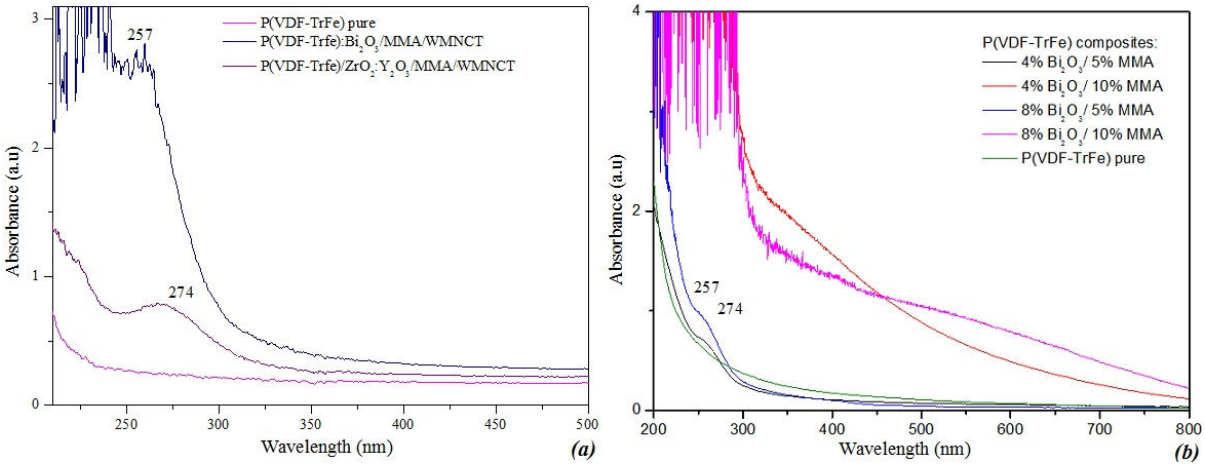

Figure 4: UV-Vis absorbance spectra for *(a)* P(VDF-TrFE) pure matrix, P(VDF-TrFE)/ZrO_2:Y_2O_3/MMA/MWNCT and P(VDF-TrFE)/Bi_2O_3/MMA/MWNCT composites; *(b)* P(VDF-TrFE)/Bi_2O_3/MMA composites with different concentrations surface modifier (MMA) to 4 and 8 wt% Bi_2O_3.

Figure 4 *(a)* investigates the optical changes induced by the addition of metal attenuator and MWNCT into the polymeric matrix by UV-Vis spectra for pristine P(VDF-TrFE), P(VDF-TrFE):Bi_2O_3/MMA/cheaptube MWNCT and P(VDF-TrFE)/ZrO_2:Y_2O_3/MMA/cheaptube MWNCT composites. The pure polymer matrix presents optical transparency in the UV-Vis range. On the other hand, there are the increase of the absorbance for the composites that introduced metals attenuators and the carbon nanotubes. In Figure 4 *(b)* investigates the optical changes induced by the addition of Bi_2O_3 nanoparticles into the P(VDF-TrFE)/Bi_2O_3/MMA composites with different concentrations surface modifier (MMA). The concentration of 10:1 MMA presented saturation which may be related to the increase of porosity of the sample with increase of the methacrylic acid. These overlapped absorption bands are attributed to the sum of the p - p* transitions of PMMA absorption band, which starts around 270nm and attains its maximum at 226 nm [6,7]. The overall absorbance observed for wavelengths ranging from 400nm to 800 nm, in both UV-Vis graphics *(a)* and *(b)*, indicates that the composites are totally transparent in this visible spectral region. The transparent protective garments can be very useful during interventional procedures in order to control the damage levels to patient skin provoked by the incident X-rays.

In general, changes in optical absorption are brought about by the formation of stable free radicals and double bonds C=C and conjugates (doublets and triplets), appearing well defined in the excitation spectra between 180 and 500 nm [6,7]. In the doublets there is the formation of alternating double bonds between single carbon bonds, and as these conjugates increase, the transition energy $\pi \rightarrow \pi^*$ decreases, indicating the extent of the degradation process. In both UV-Vis spectras, *(a)* and *(b)*, shows the peaks corresponding to triplet formation at 257 and 274 nm that can be attributed to synthesis process of composites.

Thermal analyzes by DSC were performed to observe if there were changes in the transition phases and loss of crystallinity during the synthesis of the composites with the presence of the MWCNT nanotube, Table 1. During heating it is observed that the two endothermic peaks are present corresponding to the ferro-paraelectric transition at the lowest temperature,

termed the Curie Temperature (T_c), and the melt phase transition (T_M), at the highest temperature, of the copolymer.

Table 1: Thermal analysis of nanocomposites

P(VDF-TrFe) matrix		T_M (°C)	L_M (J.g^{-1})
Bi_2O_3 /MMA composites	0.25% cheaptube MWNCT	149.25	24.83
	0.75% cheaptube MWNCT	149.59	16.55
ZrO_2:Y_2O_3 /MMA composites	0.25% cheaptube MWNCT	149.44	25.06
	0.75% cheaptube MWNCT	150.89	23.29
Pristine composites	0.75% cheaptube MWNCT	150.09	24.51
Pristine composites	0.25% 3100 MWNCT	147.91	24.31
Bi_2O_3 /MMA composite		149.49	23.99
Bi_2O_3 composite		150.80	25.42
ZrO_2:Y_2O_3 /MMA composite		151.13	21.65
Pristine (pure matrix)		151.22	26.59

On cooling, can be observed the exothermic peaks associated with the crystallization process at the highest temperature and the para-ferroelectric phase transition at the lowest temperature. These two phase transitions are reversible and present thermal hysteresis. In the melt transition, the latent heat of fusion (L_M) can be measured and it is associated with the crystalline volume present in the sample. In the melting the polymer chains leave their crystalline structures. Thus, if there is a reduction in the crystallinity of the polymer, there will also be a decrease in the L_M because it measures the amount of heat required to carry out the melt phase transition. In table 1, the P (VDF-TrFe) copolymer has a higher crystalline volume, as expected. Composites filled with Zirconia stabilized by yttria showed a greater reduction of the value latent heat in relation to bismuth oxide and, consequently, lower the crystalline volume. The presence of methacrylic acid reduced of the value latent heat. There is not a significantly reduce of the value latent heat in the composites with 0.25% cheaptube. On the other hand, there is a significant reduction in the latent heat value when the nanotube concentration is increased to 0.75%.

3.2. Attenuation radiation of composites

Bismuth oxidation composites showed a better attenuation factor compared to Zirconia stabilized by yttria composites, as shown in Figure 5. The presence of nanotube contributed to the increase of attenuation, in 7.14% for Bi_2O_3 composites and 6.5 % for ZrO_2:8%Y_2O_3 composites.

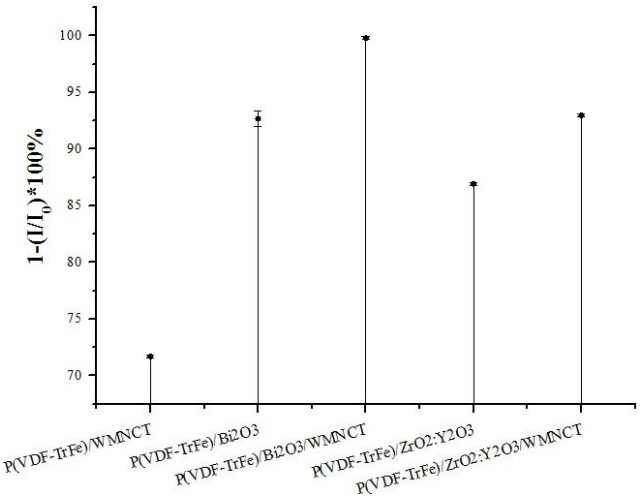

Figure 5: X-ray beam attenuation of P(VDF-TrFE) composites normalized to 100 µm for 8.047 keV monoenergetic photons

In the attenuation factor studied, the difference between the solvents diluted in the nanotubes was only 0.73% for cheaptube WMNCT. This result is within the error range of 0.15, that indicates that there was no interference in the type of solvent applied to the nanotube for DMAc or DMF. The difference between the nanotube concentration, nanotube type and the presence of methacrylic acid in the attenuation factor also was studied, as shown in Table 2. The presence of MMA did not interfere with the attenuation factor. The increase in nanotube concentration does not significantly improve the attenuation factor.

Table 2: Attenuator Composites

P(VDF-TrFe):Bi_2O_3 composites		Attenuation (%)
10:1 MMA	0.25% cheaptube MWNCT	97,50 ± 0,16
	0.75% cheaptube MWNCT	99,81 ± 0,14
10:1 MMA	0.25% 3100 MWNCT	92,83 ± 0,68
	0.75% 3100 MWNCT	96,14 ± 0,13
0:1 MMA	0.25% cheaptube MWNCT	97,14 ± 0,14

3. CONCLUSIONS

P(VDF-TrFE) composites filled with Bi_2O_3/MAA and ZrO_2:Y_2O_3/MMA with the introduction of the 3100 and cheaptube multiple-walled carbon nanotubes were produced by casting. UV-Vis spectroscopic data indicates that all composites these work are transparent in the 400-800nm visible spectral region. Carbon triplets at 257 and 274 nm were visualized in the spectra that can be attributed to synthesis process of composites. From the thermograms, composites filled with ZrO_2:Y_2O_3/MMA showed lower the crystalline volume in relation to bismuth oxide Bi_2O_3/MAA. DSC data evinced a gradual decrease in the crystalline volume of the polymer composites for increased to 0.75% of the WMNCT.

Radiation shielding characterization for 8.047 keV monoenergetic photons demonstrates that composites filled with ZrO_2:Y_2O_3 and Bi_2O_3 at 8 wt% can attenuate above 85% of the X-rays beam. The presence of nanotube contributed to the increase of attenuation, in 7.14% for Bi_2O_3 composites and 6.5 % for ZrO_2:8%Y_2O_3 composites. This energy range may correspond to scattered radiation arriving at some more radiosensitive organ near the irradiated area during a radiological medical procedure. In this case, the composite would be indicated to attenuate this radiation. These results indicate that these polymer composites are good candidates to be explored as light-weighted and flexible protective shielding for application in radiological procedures.

ACKNOWLEDGMENTS

This work was supported by Conselho Nacional de Desenvolvimento Científico e Tecnológico (CNPq), Fundação de Amparo à Pesquisa do Estado de Minas Gerais (FAPEMIG) and Comissão Nacional de Energia Nuclear (CNEN).

REFERENCES

1. M. Brambilla, G. Marano, M. Dominietto, A. R. Cotroneo , A. Carriero, "Patient radiation doses and references levels in interventional radiology", *Radiol Med.,* **v.107**, nº4, pp. 408-418 (2004).

2. D. J. Mclaughlin, R. B. Mooney, "Dose reduction to radiosensitive tissues in CT. Do commercially available shields meet the users' needs?", *Clinical Radiology*, **v.59**, pp. 446–450, (2004).

3. B. F. Wall, "Radiation protection dosimetry for diagnostic radiology patients",*Radiation Protection Dosimetry*, **v.109**, p. 409-419 (2004).

4. Trianni, G. Chizzola, H. E. Toh, E. Quai, G . Cragnolini, A. Bernardi, R. Proclemer, H. Padovani, "Patient skin dosimetry in haemodynamic and electrophysiology interventional cardiology", *Radiat. Protection Dosimetry*, **v.117**, pp. 241-246 (2005).

5. S. Nambiar, J. T. W. Yeow, "Polymer-Composite Materials for Radiation Protection", *ACS Appl. Mater. Interfaces,* **v.4**, pp. 5717−5726 (2012).

6. C. C. P. FONTAINHA, L. O. Faria, A. T. BAPTISTA NETO; A. P. SANTOS, "P(VDF-TrFE)/ZrO_2 Polymer-Composites for X-ray Shielding", *Materials Research*, **v. 19**, pp. 91-99, (2016).

7. C. C. P. FONTAINHA, L. O. Faria, A. T. BAPTISTA NETO, "Polymer-based Nanocomposites of P(VDF-TrFE)/Bi_2O_3 Applied to X-ray Shielding", *Research & Reviews: Journal of Material Science*, **v. 4**, p. 16-23, (2016).

8. T. FUJIMORI, S. TSURUOKA, B. FUGETSU, S. MARUYAMA, A.TANIOKA, M.TERRONES, M. DRESSELHAUS, M. ENDO, K. KANEKO,"Enhanced X-Ray Shielding Effects of Carbon Nanotubes", Materials Express, v.1, nº 4, 273-278 (2011).

9. P. PERIASAMY,S.YANG, S.CHEN, "Preparation and characterization of bismuth oxide nanoparticles-multiwalled carbon nanotube composite for the development of horseradish peroxidase based H2O2 biosensor", *Talanta*, **v.87**, pp.15-23, (2011).

10. J. Viegas, L. A. Silva, A. M. S. Batista, C. A. Furtado, J. P. Nascimento[3], L. O. Faria, "Increased X-ray Attenuation Efficiency of Graphene-based Nanocomposite", Ind. & Eng. Chem. Research, (2017), in print.